

0.04% change in C . A shift of 1:1000 of the P_1 caused only a 0.05% change in B and a 0.13% change in C . Thus, a small systematic error in the piston area does not make an important change in the virial coefficients when the direct method is used.

In the apparatus constant method the value of the constant at zero pressure must be determined very precisely. Errors in this constant introduce an error in the compressibility factor which increases as the number of expansions increase. The method of determining the constant using helium in a pressure range where fourth virials are negligible is shown in Figure 1. The proper selection of the zero pressure constant is indicated by a linear relationship resulting. Unfortunately, the deviations from linearity are shown most sensitively by the low pressure points and these points are most influential in determining the constants as shown in Figure 1. As has been discussed above these points are the least accurate and may have a systematic error. The scatter in these points is considerably dampened in the apparatus constant method since the compressibility factors at which they are determined are calculated from higher pressures in the expansion. However, even a small systematic error in these points will cause a significantly erroneous choice of the apparatus constant necessary to linearize them. Since the lower pressures are generally too high, this causes the second virial coefficient, as given by the intercept in Figure 1, to be too large. In almost every case the second virials of the apparatus constant method are larger than those predicted by the direct method.

Because many of the difficulties in the apparatus constant method are avoided, the direct method proposed here is the more accurate procedure for the determination of virial coefficients from Burnett data. The data obtained by Canfield are very accurate over a wide pressure range and the pressure at which the systematic errors begin is quite low. Consequently the results of the two methods for these data are very close. If all pressures could be determined with equal relative accuracy with no nonrandom deviations at low pressures, then the results of the two methods should be identical.

ACKNOWLEDGMENT

This work was sponsored by the National Science Foundation under Grant No. G-15360 for study of the thermo-

dynamic properties of low molecular weight gases at high pressures and low temperatures. The authors would also like to acknowledge the assistance of G.S. Dawkins in the statistical analysis of the data. The authors acknowledge the assistance of Computer Labs., Inc., Houston, Texas, in making the computations.

LITERATURE CITED

- (1) Burnett, E.S., *J. Appl. Mech., Trans. ASME* **58**, A136 (1936).
- (2) Cook, D., *Can. J. Chem.* **35**, 268 (1957).
- (3) Canfield, F.B., Ph.D. Thesis, Rice University, Houston, Texas, 1962.
- (4) Canfield, F.B., Leland, T.W., Kobayashi R., *Advan. Cryog. Eng.* **8**, p. 146, Plenum Press, New York, 1963.
- (5) Danon, F., Pitzer, K.S., *J. Chem. Phys.* **36**, 425 (1962).
- (6) Hill, T.L., "An Introduction to Statistical Thermodynamics," p. 261, Addison-Wesley, Reading, Mass., 1960.
- (7) Holborn, L., Otto, J., *Z. Phys.* **23**, 77 (1924).
- (8) *Ibid.* **33**, 1 (1925).
- (9) Keesom, W.H., "Helium", Elsevier, Amsterdam, (1942).
- (10) Kramer, G.M., Miller, J.G., *J. Phys. Chem.* **61**, 785 (1957).
- (11) McGlashan, M.L., Potter, D.J.B., *Proc. Roy. Soc. (London)* **A267**, 478 (1962).
- (12) Madansky, A., *J. Am. Stat. Assn.* **54**, 173 (1959).
- (13) Michels, A., Wouters, H., *Physica* **8**, 923 (1941).
- (14) Michels, A., Wouters, H., DeBoer, J., *Ibid.* **1**, 587 (1934).
- (15) Mueller, W.H., Leland, T.W., Jr., Kobayashi, R., *A.I.Ch.E.J.* **7**, 267 (1961).
- (16) Pfefferle, W.C., Goff, J.A., Miller, J.G., *J. Chem. Phys.* **23**, 509 (1955).
- (17) Putnam, W.E., Kilpatrick, J.E., *J. Chem. Phys.* **21**, 951 (1953).
- (18) Schneider, W.G., *Can. J. Res.* **27B**, 339 (1949).
- (19) Schneider, W.G., Duffie, J.A.H., *J. Chem. Phys.* **17**, 751 (1949).
- (20) Scott, R.L., Dunlap, R.D., *J. Phys. Chem.* **66**, 639 (1962).
- (21) Silberberg, I.H., McKetta, J.J., Kobe, K.A., *J. CHEM. ENG. DATA* **4**, 314, 323 (1959).
- (22) Verschoyle, T.T.H., *Proc. Roy. Soc. (London)* **A111**, 522 (1926).
- (23) White, D., Ohio State University, *Eng. Exp. Sta. News* **24**, No. 3, 12 (1952).
- (24) White, D., Rubin, T., Camky, P., Johnson, H.L., *J. Phys. Chem.* **64**, 1607 (1960).
- (25) Young, H.D., "Statistical Treatment of Experimental Data," McGraw-Hill, New York, 1962.

RECEIVED for review January 24, 1964. Accepted April 16, 1964.

Thermoanalytical Study of Lithium Chlorate

MEYER M. MARKOWITZ, DANIEL A. BORYTA, and HARVEY STEWART, Jr.
Foote Mineral Co., Exton, Penn.

ELUCIDATION of the trends in thermal stability and of those chemical and physical processes occurring during the pyrolysis of the alkali metal (M) perchlorates has been facilitated through application of differential thermal analysis (DTA) and of thermogravimetric analysis (TGA) (39). In contrast, the alkali metal chlorates appear not to have been studied systematically by the use of these techniques. Accordingly, the present investigation of the thermal decomposition of LiClO_3 was undertaken with the views in mind of gauging the applicability of DTA and of TGA in this area, of defining the order of thermal

stability of the lithium compounds of chlorine-containing oxyanions (ClO_x^- , $x = 1, 2, 3, 4$), and ultimately, of determining the pyrolysis relationships among the alkali metal chlorates in general.

EXPERIMENTAL

Thermoanalytical Techniques. DTA experiments to about 700° were performed in a closed muffle furnace with equipment previously described (35, 39, 44) in conjunction with calibrated chromel-alumel thermocouples (24 B. and S. gage) and quartz sample tubes (3 inches \times 1/2 inch o.d.

The pyrolysis of LiClO_3 was studied by differential thermal analysis and thermogravimetry at a heating rate of $4^\circ/\text{min.}$, and by isothermal experiments at 339° . The decomposition was shown to follow the sequence: (rapid; ca. $365\text{--}430^\circ$) $\text{LiClO}_3 \rightarrow \text{LiCl} + 3/2\text{O}_2$ concomitant with $\text{LiClO}_3 \rightarrow 3/4\text{LiClO}_4 + 1/4\text{LiCl}$, and (slow; ca. $430\text{--}490^\circ$) $\text{LiClO}_4 \rightarrow \text{LiCl} + 2\text{O}_2$. Estimates are presented for ΔH_f° (LiClO_3) and ΔF_f° (LiClO_3) at 25° , thereby permitting tabulations of the standard enthalpy and free energy changes at 25° for a number of the processes occurring during the pyrolysis of the alkali metal chlorates in general. These data suggest the occurrence of internal oxygenation effects in decomposing chlorate melts leading to the formation of the more thermodynamically and kinetically stable perchlorates, viz., $\text{MClO}_3 + 1/2\text{O}_2 \rightarrow \text{MClO}_4$. Trends in the thermal stabilities of the alkali metal compounds of chlorine-containing oxyanions (MClO_x , $x = 1, 2, 3, 4$) are detailed and the following order of stabilities is demonstrated: $\text{MClO}_4 > \text{MClO}_3 > (\text{MClO}_2, \text{MClO})$.

$\times 1\frac{1}{2}$ inch i.d.) concentric with larger Pt tubes used to provide more uniform heat distribution. For those runs carried out to only 180° , a method used earlier (32) was adopted in combination with a liquid heat transfer medium (550 Silicone Fluid, Dow-Corning Corp., Midland, Mich.). Visual observation of the sample was possible during these heatings.

TGA determinations were made with apparatus already detailed (33, 44) using Vycor sample tubes. Appropriate corrections were applied to all measured temperatures (34) to approximate the sample temperature from the furnace temperature.

Each DTA and TGA experiment was conducted under a dry, flowing Ar atmosphere and, unless otherwise specified, one gram samples were used and subjected to a linear heating rate of $4^\circ/\text{minute}$ (38).

Materials and Chemical Analytical Procedures. Anhydrous LiClO_3 was prepared by the method of Potilitzin (52) involving the double decomposition of equivalent quantities of Li_2SO_4 and $\text{Ba}(\text{ClO}_3)_2$ in aqueous solution. The solid product obtained after evaporation of water was dried at 100° under 1 micron Hg pressure for two days. The material was stored over P_2O_5 and all handling and manipulation of the highly deliquescent LiClO_3 was performed in a glove box under dry Ar or N_2 . Analyses: Cl as ClO_3^- : found, 39.08% (calcd., 39.24%); Cl as Cl^- : found, 0.02%. Spectrographic examination showed the presence of < 5 p.p.m. Al, < 5 p.p.m. Ca, < 1 p.p.m. Cu, < 1 p.p.m. Mg, < 0.5 p.p.m. Mn, and < 1 p.p.m. Ni; B, Cr, Pb, Sn, Ti, and V were absent.

Partially decomposed residues of LiClO_3 were analyzed for Cl^- , ClO_3^- , ClO_4^- , and O^{2-} contents, except for several instances where ClO_4^- was taken by difference. Cl^- was determined gravimetrically as AgCl ; ClO_3^- was assayed as additional Cl^- after reduction of the sample aliquot with aqueous SO_2 . ClO_4^- was analyzed by precipitation as nitron perchlorate (58) after reduction of ClO_3^- . O^{2-} content was found by titration to the phenolphthalein end-point with $0.1N$ HCl.

The total Cl_2 evolved from various reacting samples was determined by absorption in KI solution as described previously (44).

X-ray diffraction powder patterns of products from LiClO_3 -condensed phosphate reaction mixtures were obtained with a General Electric XRD-5 diffractometer using Ni-filtered Cu-K_α radiation.

RESULTS

Thermal Behavior of LiClO_3 up to 180° . The polymorphism of LiClO_3 has been a matter of some dispute in the literature. Some workers (29) have claimed the reversible crystallographic changes $\gamma \rightleftharpoons \beta$, $\beta \rightleftharpoons \alpha$ at 44.5° and 106.4° , respectively, whereas others (3, 10) have reported but a

single crystallographic transition at about 100° . Accordingly, in the present study, DTA patterns of LiClO_3 on an expanded scale were obtained over the temperature range from ambient to about 180° . Only a single transition occurring at 111.1° was ever found upon repeated heating and cooling cycles. A second endotherm was identified by visual observations as the melting point of $\alpha\text{-LiClO}_3$ and agrees (129.2°) with previously reported values (3, 10, 8, 48, 52). These changes are seen as the first two endotherms in the DTA curves of Figures 1 and 2. Supercooling of liquid LiClO_3 and of $\alpha\text{-LiClO}_3$ by as much as 50° was observed in the course of the present experiments.

The LiClO_3 samples subjected to the above DTA studies showed no changes in composition after the runs as determined by chemical analyses; this, of course, was also indicated by the reproducibility of the invariant points despite repeated thermal cycling. Maintaining fused LiClO_3 at 135° for two days under an Ar atmosphere at ambient pressure resulted in no measurable degree of decomposition as revealed by chemical analyses. These observations would indicate the feasible use of LiClO_3 as a stable component in phase studies of anhydrous salt systems at moderately elevated temperatures as have been performed with LiClO_4 (32, 36, 39, 41).

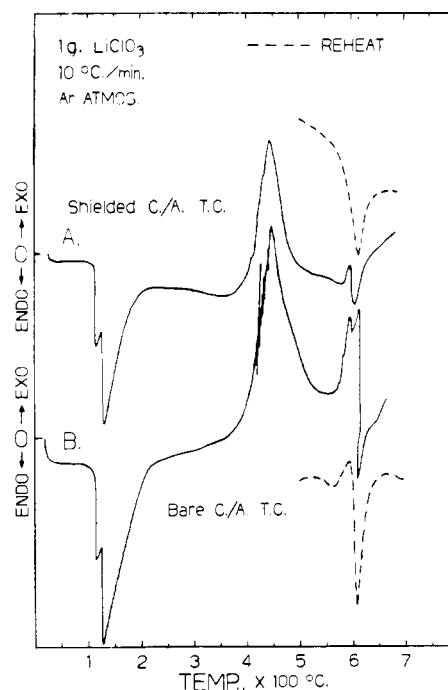
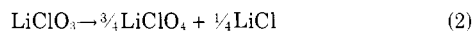
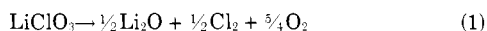


Figure 1. DTA curves of LiClO_3 heated at $10^\circ/\text{Min.}$

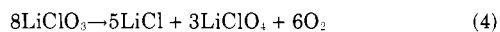
The density of α -LiClO₃ at room temperature was measured as 2.631 by a gas pycnometer method.

Isothermal Decomposition Studies of LiClO₃ at 339°. Some preliminary information on the thermal decomposition of LiClO₃ was secured by maintaining 4–5 gram samples at 339° ± 1° under flowing Ar for varying periods of time. The analyses of these residues are presented in Table I in terms of the extents of decomposition (x_i) of LiClO₃ as per the reactions:



Equation 2 is customarily used to account for MClO₄ formation in MClO₃ melts (1, 12, 13), although an alternate formulation of the reaction will be suggested in a later section of this paper.

The data of Table I indicate a number of interesting aspects of the pyrolysis of LiClO₃. Both Reactions 2 and 3 appear to be catalyzed as the degree of LiClO₃ decomposition increases. This autocatalytic behavior is akin to that observed for the disproportionation of KClO₃ (21, 50) and for oxygen evolution from various KClO₃-KCl mixtures (21). For LiClO₃, Reactions 2 and 3 seem to occur at approximately the same rates as suggested by the relative constancy of the ratio $1.5 > x_2/x_3 \geq 1.0$ up to 12 hours of heating. After 12 hours, the decomposition residue is substantially a mixture of LiCl and LiClO₄ in a 5:3 mole ratio. Thus, the pyrolysis of LiClO₃ after this interval can be closely represented by the overall equation:



which is the sum of Equations 2 and 3. About one-half of the oxygen loss occurs subsequently through the considerably slower reaction:



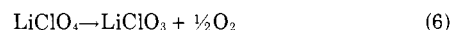
when the melt is devoid of any appreciable LiClO₃ content.

The rate of decomposition of LiClO₄ in a saturated solution of LiCl in LiClO₃ at 339° may be computed (36) and is found to be only 0.41% per hour, so that the aug-

menting LiCl content due to Reaction 5 becomes significant only after the longer heating periods. In Table I, Reaction 5 was not considered to cause any alterations in x_2 and x_3 although it clearly plays a role after the 12-hour heating period when the LiClO₄ content has reached a maximum. This effect is manifested in the steadily decreasing magnitude of x_2/x_3 beyond the 12 hour interval. Indeed after this point, the thermal decomposition of LiClO₃ is essentially complete so that the succeeding values of x_i are merely formal in nature and the changes in the system are best represented by Equation 5.

The values of x_3 calculated from the chemical analyses agreed closely with those values computed from the weight losses. This would be expected because of the generally small magnitude of x_1 . Other studies (16, 20) have shown the occurrence of small degrees of Cl₂ evolution from KClO₃ and from various KClO₃-catalyst mixtures as well as from combusting NaClO₃-Fe compositions (54). It is clear then that full kinetic scheme for the pyrolysis of these MClO₃ compounds would have to take into account a reaction such as that represented by Equation 1.

When LiClO₄ was heated under flowing Ar at 399° ± 1° for 72 hours 0.38% decomposed following Equation 5 and 0.20% decomposed as per:



These results together with those obtained previously show that LiClO₄ is appreciably more thermally stable than is LiClO₃. Consequently, it was anticipated that this marked difference in decomposition rates would be reflected in the DTA and TGA patterns for LiClO₃.

High Temperature DTA Patterns of LiClO₃. DTA patterns were obtained for LiClO₃ at a heating rate of 10°/minute using thermocouples shielded in an outer, close-fitting quartz tube. A typical curve is presented in Figure 1a. The exothermal decomposition band starts to depart appreciably from the baseline at about 376° and consists of only a single, smooth peak. There are no discontinuities in this band indicative of the occurrence of reactions of widely differing rates, e.g., Reactions 2 and 3 as compared with Reaction 5. Accordingly, an attempt was made to secure better resolution in the DTA curves by the use of bare thermocouples (2, 18); the behavior found by this procedure is shown in Figure 1b. Here, the steadily rising baseline after fusion would indicate the occurrence of slow decomposition at lower temperatures than in the previous experiment with the rate becoming appreciable at about 370°. As seen in Figure 1b, again only a single large exotherm was recorded. However, through use of a heating rate of 4°/min. (Figure 2a), a knee appeared on the decomposition exotherm; a similar effect occurred with the use of a bare thermocouple (Figure 2b). It was felt that this discontinuity was associated with the final portion of the decomposition sequence of LiClO₃, i.e., Reaction 5. As in the instance of the higher heating rate, the use of bare thermocouples resulted in the onset of rapid decompo-

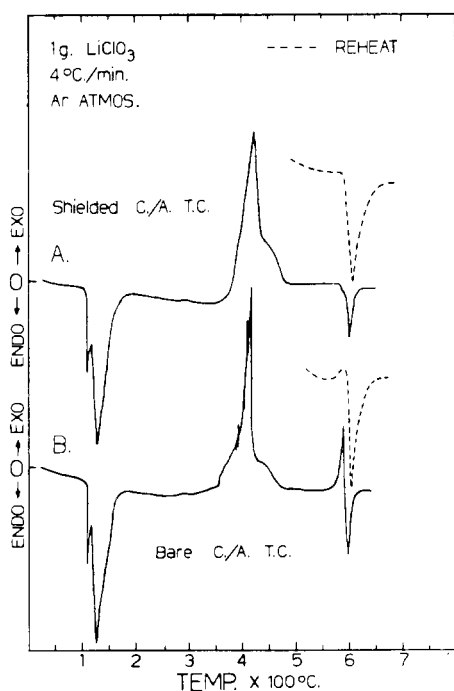


Figure 2. D.T.A. curves of LiClO₃ heated at 4°/min.

Table I. Decomposition Paths of LiClO₃ at 339 ± 1°

Time, Hrs.	Mole Fraction LiClO ₃ Remaining	x_1	x_2	x_3	x_2/x_3
1	0.9483	0.0000	0.0260	0.0257	1.012
3	0.8700	0.0000	0.0769	0.0531	1.448
5	0.6693	0.0008	0.1899	0.1400	1.356
7	0.4794	0.0012	0.2861	0.2333	1.226
8	0.3807	0.0046	0.3184	0.2963	1.075
10	0.2972	0.0032	0.3558	0.3438	1.035
12	0.2401	0.0064	0.3807	0.3728	1.021
16	0.0294	0.0066	0.3828	0.5812	0.659
24	0.0041	0.0026	0.3590	0.6343	0.409
64	0.0057	0.0088	0.2452	0.7403	0.331

sition at lower temperatures (355°) than with the shielded thermocouples (367°). It is pertinent to note the considerable oscillations in ΔT shown in the decomposition regions of Figures 1b and 2b.

The explanation for the differences observed for the two types of thermocouple arrangements was traced to the attack of the bare metals by the sample melt. Qualitative analyses (17) of decomposed residues from DTA runs showed the presence of soluble Cr and Ni compounds as well as black solid particles of metal oxides in only those samples in which bare thermocouples had been immersed. Thus, the use of unshielded thermocouples in these experiments must give rise to both homogeneous and heterogeneous catalysis of the decompositions of LiClO_3 and of LiClO_4 , thereby introducing additional experimental complications. The application of bare thermocouples is feasible when there is no likelihood of sample-thermocouple interactions (42). The promotion of the pyrolysis of LiClO_3 by chromel-alumel couples was also demonstrated by isothermal studies in LiClO_3 melts with and without the presence of composite wire spirals.

A partial cause of the poor development of the second exotherm in the decomposition region of LiClO_3 may be found by examination of the final endotherms in Figures 1 and 2 attributable to the fusion of the major residual reaction product, LiCl (m.p., 614°). In each of these curves, the fusion endotherm is much smaller during the first heating than during the second heating and, in some instances, is actually preceded by an exotherm in the initial heating. This type of behavior would indicate that the thermocouple is initially in contact with only a fraction of the LiCl formed as a result of decomposition and that after the initial fusion, the amount of LiCl in the region of the thermocouple is augmented. Visual observations of the samples in the temperature interval between the beginning and the end of rapid decomposition (*i.e.*, after complete conversion to solid LiCl) showed that the turbulence of the pyrolysis reactions had caused the sample to overflow the holder and to be distributed over the entire inner surface of the containing tube. This resulted in a diminution of the mass of material in the vicinity of the thermocouple and in poor thermal contact between sample and sensor (35). These effects appeared to be more pronounced at the higher heating rate (Figure 1); at the lower heating rate (Figure 2), there was sufficient sample retained in the bottom of the quartz holder after the first stage of LiClO_3 decomposition (Reaction 4) to give indications of the second exotherm (Reaction 5). The use of still lower heating rates (1° and 2°/min.) or of a smaller sample size (0.5 g.), and a wider sample holder (one inch) at a heating rate of 4°/min. somewhat improved the development of the second exotherm but also decreased the areas bounded by all the breaks. The exotherms prior to LiCl fusion are due to enhanced thermal conductivity because of liquid phase formation causing better thermocouple-sample contact and furnace-sample heat transfer. This type of behavior has been observed in other systems undergoing fusion phenomena during DTA (5).

An interrupted DTA run was carried out to the first peak temperature indicated in Figure 2a (425°) and the quenched residue was analyzed. It contained (mole %) 0.88% LiClO_3 , 0.55% Li_2O , 68.24% LiCl , and 30.33% LiClO_4 (by difference). Clearly then the second exotherm (Figure 2a) could be associated with the thermal decomposition of LiClO_4 (Reaction 5). The mole ratio of LiCl to LiClO_4 at this point was 2.25 rather than 1.67 as expected from the isothermal runs at 339°. However, as will be seen subsequently, the complementary TGA experiments on LiClO_3 closely fulfilled the anticipation of two distinct stages in the pyrolysis of LiClO_3 under these experimental conditions (*viz.*, Equations 4 and 5). A sharper resolution

of these two levels of reaction was not possible by DTA because of the combined effects of sample turbulence, of large thermal gradients, and perhaps most importantly, of the overlapping of exothermic breaks due to successive reaction. This last occurrence causes a continuation of the first peak due to the start of the second succeeding exotherm. As will be shown later, a large degree of thermal overlap probably occurs at the higher heating rate, which in addition to increased sample turbulence over the lower heating rate, causes virtually complete obscurity of the heat release from Reaction 5.

TGA Pattern of LiClO_3 . Figure 3a illustrates a typical TGA curve for LiClO_3 . The rate of weight loss becomes appreciable at about 370° and is followed by a marked decrease in rate at about 430° where the aggregate weight loss is 27.7%. This weight loss corresponds closely to that expected for Equation 4, *i.e.*, $8\text{LiClO}_3 \rightarrow 5\text{LiCl} + 3\text{LiClO}_4 + 6\text{O}_2$ (calcd. weight loss, 26.6%). The subsequent reaction period (ca. 430–490°) would then be related to Reaction 5, *i.e.*, $\text{LiClO}_4 \rightarrow \text{LiCl} + 2\text{O}_2$. This latter reaction proceeds more rapidly than for pure LiClO_4 due to autocatalysis provided by the LiCl from the preceding reaction (33, 36, 37). TGA experiments with pure LiClO_4 show rapid decomposition to ensue at about 445°.

A 1.0905 gram sample of LiClO_3 was heated in the TGA apparatus to the loss of 0.2925 gram (calcd. for 50% loss of available O_2 , 0.2896 gram). The quenched residue was analyzed for LiClO_3 and LiCl contents and in conjunction with the weight loss data the following assay was obtained (mole %): 2.40% LiClO_3 , 1.97% Li_2O , 57.25% LiCl , and 38.37% LiClO_4 . The mole ratio of LiCl to LiClO_4 is thus 1.49, in fairly good agreement with that (1.67) to be predicted from the occurrence of Reactions 2 and 3 to equal extents, *i.e.*, Equation 4.

The total weight loss suffered by LiClO_3 (Figure 3a) is 102.6% of that based on completion of Reaction 3, *i.e.*, $\text{LiClO}_3 \rightarrow \text{LiCl} + \frac{3}{2}\text{O}_2$. Inasmuch as earlier experiments had indicated the presence of Li_2O in decomposed LiClO_3 residues, the augmented weight loss could be accounted for by the occurrence of Reaction 1, $\text{LiClO}_3 \rightarrow \frac{1}{2}\text{Li}_2\text{O} + \frac{1}{2}\text{Cl}_2 + \frac{5}{4}\text{O}_2$, to the extent of 3.8%. Direct determination of the total amount of Cl_2 evolved from the decomposition of LiClO_3 indicated Reaction 1 to occur to the extent

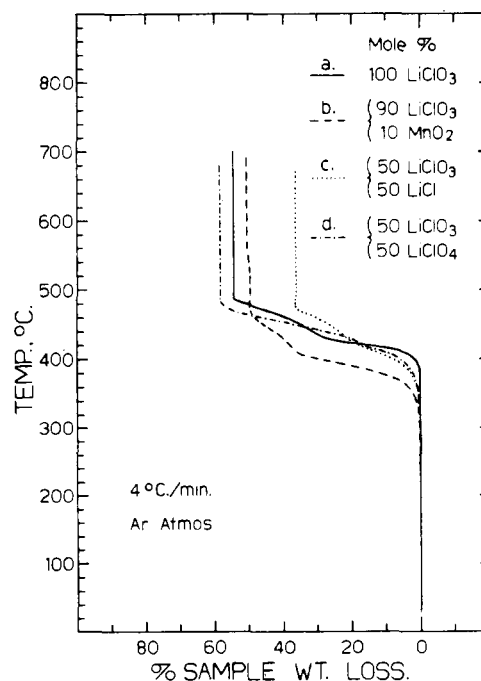


Figure 3. TGA curves of LiClO_3 and of some LiClO_3 -containing mixtures

of 4.5%. As will be demonstrated later, the ability of LiClO_3 to yield Li_2O on thermal decomposition constitutes the foundation for its use as an elevated temperature base in reactions with acidic or oxide ion deficient materials.

Note that the TGA curve for LiClO_3 up to 430° reflects principally the occurrence of Reaction 3 because Reaction 2 does not engender any change in sample weight, whereas the DTA curve over the same temperature range manifests the composite results of the heat release from both Reactions 2 and 3.

Thermal Behavior of Some LiClO_3 -Containing Mixtures.
90 Mole % LiClO_3 -10 Mole % MnO_2 . As is known for KClO_3 (7, 9, 20), it was found for LiClO_3 that MnO_2 causes the acceleration of O_2 evolution. This effect may be seen from Figures 3b and 4a where the onset of rapid decomposition of LiClO_3 occurs at about 330° . From both the DTA and TGA curves it appears that the quantity of LiClO_4 formed by Reaction 2 is diminished by the presence of the MnO_2 . Thus, the second exothermic break in Figure 4a is smaller than for pure LiClO_3 and the inflection at 406° in the TGA curve (Figure 3a), attributable to the onset of rapid pyrolysis of LiClO_4 , occurs at a weight loss (72.8% of that based on Reaction 3) indicative of about 25% conversion of LiClO_3 to LiClO_4 , rather than 50% as for Reaction 2. It appears then that the effect of MnO_2 is to catalyze chloride formation over perchlorate formation.

The catalytic action of a 10 mole % addition of MnO_2 to LiClO_3 results in the lowering of the start of rapid decomposition to about 402° .

50 MOLE % LiClO_3 -50 MOLE % LiCl . Both the DTA (Figure 4b) and TGA (Figure 3c) patterns indicate that the onset of rapid decomposition of LiClO_3 is lowered to about 343° by the presence of the LiCl . From the TGA curve it is seen that the LiCl appears to catalyze both O_2 evolution and LiClO_4 formation inasmuch as the inflection in rate of weight loss at 422° corresponds to the completion of Reaction 3 to 55.5%; the succeeding portion of the TGA curve is, of course, attributed to the decomposition of the LiClO_4 content (Reaction 5).

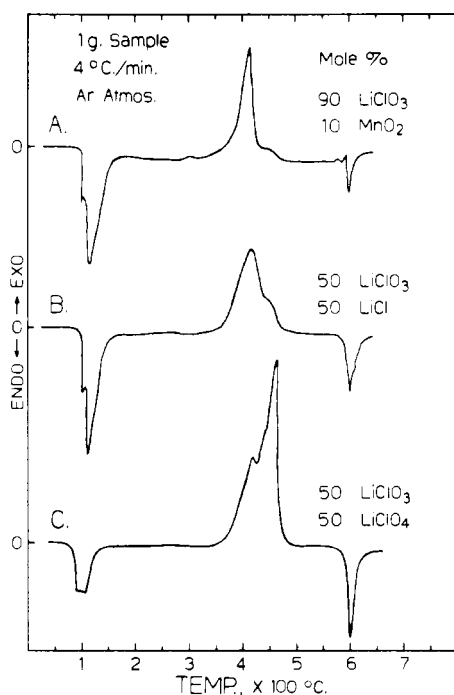
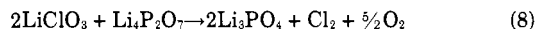
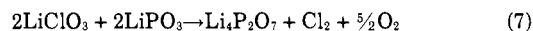


Figure 4. DTA curves of some LiClO_3 -containing mixtures

50 MOLE % LiClO_3 -50 MOLE % LiClO_4 . Decomposition phenomena are seen to ensue at about 350° from both the DTA (Figure 4c) and TGA (Figure 3d) runs. The DTA curve shows the second exotherm to be considerably augmented over pure LiClO_3 as would be expected from the increased LiClO_4 content of the sample. The initial endotherm at about 100° corresponds to liquid phase formation in this binary mixture as observed visually with a separate sample.

LiClO_3 -CONDENSED PHOSPHATE MIXTURES. It was thought that as in the instance of LiClO_4 (44), LiClO_3 might prove effective as a depolymerizing agent for condensed lithium phosphates (e.g., $\text{Li}_4\text{P}_2\text{O}_7$ and the polymeric LiPO_3) through its decomposition as per Reaction 1 which yields O^{2-} ions. Total Cl_2 evolution and preliminary DTA and TGA studies showed reaction to become measurable at about 250° for the mixtures of Table II which also summarizes the extents of conversion of the LiClO_3 contents to Li_2O .

The formation of Li_2O in the mixtures of Table II is reflected in the disruption on the polyphosphate ions to yield simpler anionic species (30). Thus, x-ray powder patterns of the heated residues from samples 1, 2, and 3 showed the presence of $\text{Li}_4\text{P}_2\text{O}_7$ and Li_3PO_4 in samples 1 and 2 and Li_3PO_4 in sample 3; each residue showed a considerable decrease in line intensities attributable to the original condensed phosphate reactant. These x-ray data in combination with the results of Table II demonstrate the occurrence of the reactions:



Consequently, acid-displacement reactions of the type: $\text{Li}_2\text{O} \cdot \text{Cl}_2\text{O}_5 + \text{Li}_2\text{O} \cdot \text{P}_2\text{O}_5 \rightarrow (2\text{Li}_2\text{O}) \cdot \text{P}_2\text{O}_5 + \text{Cl}_2 + \frac{1}{2}\text{O}_2$ are suggested. Reactions 7 and 8 ensue at considerably lower temperature than does the thermal decomposition of LiClO_3 itself (365°), or condensed phosphate depolymerization using LiClO_4 (44), or Li_2O , LiOH , Li_2CO_3 , and Li_2O_2 as bases (40).

Corresponding types of depolymerization reactions with KClO_3 are implied by noting the increased Cl_2 evolution found in $\text{KClO}_3\text{-K}_2\text{S}_2\text{O}_7$ (16) and in $\text{KClO}_3\text{-Cr}_2\text{O}_3$ (47) mixtures. In addition, Mellor (46) and others (20) have observed the general increase in evolved Cl_2 from decomposing KClO_3 in the presence of acidic oxides.

DISCUSSION OF RESULTS

Some significant insights into the pyrolysis of MClO_3 salts in general and of LiClO_3 in particular may be gained by consideration of some of the thermodynamic quantities (ΔF^\ddagger , ΔH^\ddagger) associated with the observed chemical changes. However, as in the instances of the corresponding MClO_4 compounds (31), there is a paucity of thermodynamic data for chlorates. Accordingly, some of these values will have to be estimated (31).

ΔH^\ddagger values at 25° are available for NaClO_3 , KClO_3 , and RbClO_3 (53) and the approximate values of ΔH^\ddagger at 25° for LiClO_3 and CsClO_3 may be derived from the former data by use of a method proposed by Hoppe (27). He

Table II. Some LiClO_3 -Condensed Phosphate Reactions

Sample No.	Initial Composition, Mole %	% Conversion of LiClO_3 to Li_2O	
		TGA data	Cl_2 evolution
1	50 LiClO_3 -50 LiPO_3	99.7	94.8
2	66.7 LiClO_3 -33.3 LiPO_3	61.0	57.8
3	66.7 LiClO_3 -33.3 $\text{Li}_4\text{P}_2\text{O}_7$	48.8	50.8

established the existence of a linear relationship between the equivalent heats of formation of oxyanion compounds of noble gas-type cations (e.g., the alkali and alkaline earth metals) from the corresponding metal oxides and acid anhydrides [$\Delta R_f^\circ(M_nXO_z)$] and the difference in equivalent heats of formation between the metal chlorides and oxides. Thus, for the alkali metals:

$$\Delta R_f^\circ(M_nXO_z) = [\Delta H_f^\circ(M_nXO_z)]_{\text{equiv.}} - [\Delta H_f^\circ(M_2O)]_{\text{equiv.}} - [\Delta H_f^\circ(X_2O_3)]_{\text{equiv.}} \quad (9)$$

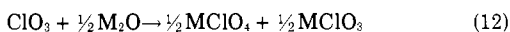
$$\Delta R_f^\circ(M_nXO_z) = A[\Delta H_f^\circ(MCl) - \frac{1}{2}\Delta H_f^\circ(M_2O)] + B \quad (10)$$

Close linearity was found to hold among various nitrates, orthophosphates, carbonates, sulfites, sulfates, and perchlorates where the appropriate data were available. Thus, knowledge of $\Delta R_f^\circ(M_nXO_z)$, $\Delta H_f^\circ(MCl)$, and $\Delta H_f^\circ(M_2O)$ for some members of a particular class of oxyanion compounds at a given temperature permits an estimate to be made of the unknown $\Delta H_f^\circ(M_nXO_z)$ for a specific compound of that class. The application of this approach to $MClO_4$ salts gives the data of Table III (26, 27), where $\Delta H_f^\circ(MClO_4)_{\text{calcd.}}$ at 25° was obtained from the equation:

$$\Delta R_f^\circ(MClO_4) = 1.124 [\Delta H_f^\circ(MCl) - \frac{1}{2}\Delta H_f^\circ(M_2O)] - 22.91 \quad (11)$$

Table III shows the close agreement secured between the literature and the calculated values for $\Delta H_f^\circ(MClO_4)$ at 25°.

Inasmuch as there is no known acid anhydride of $HClO_3$, it will be necessary to utilize as the basis for the calculation of $\Delta R_f^\circ(MClO_3)$ for $LiClO_3$ and $CsClO_3$, the reaction (55):



$\Delta H_f^\circ(ClO_3)$ and $\Delta H_f^\circ(MClO_4)$ are known as well as $\Delta H_f^\circ(MClO_3)$ for $NaClO_3$, $KClO_3$, and $RbClO_3$. These data are incorporated in Figure 5 which corresponds to the equation:

$$\Delta R_f^\circ(MClO_4, MClO_3) = 1.34[\Delta H_f^\circ(MCl) - \frac{1}{2}\Delta H_f^\circ(M_2O)] - 11.08 \quad (13)$$

Therefore,

$$\Delta H_f^\circ(MClO_3) = 2.68 \Delta H_f^\circ(MCl) - 0.34 \Delta H_f^\circ(M_2O) - \Delta H_f^\circ(MClO_4) + 2\Delta H_f^\circ(ClO_3) - 22.16 \quad (14)$$

The computed values at 25° of $\Delta H_f^\circ(MClO_3)$ are given in Table IV and are found to be in good agreement with the corresponding literature values where these are known (53).

ΔF_f° data at 25° are available for $NaClO_3$ (-59.1 kcal./mole) (28), $KClO_3$ (-69.3 kcal./mole) (53), and $RbClO_3$ (-67.8 kcal./mole) (53). These values yield an average entropy change (ΔS_f°) of 64.2 ± 3.4 e.u. for the conversion

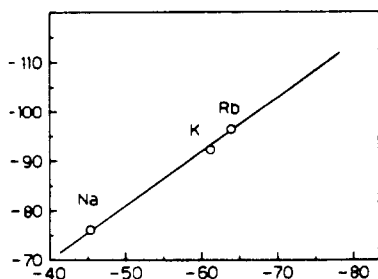


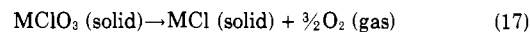
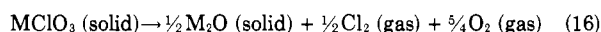
Figure 5. Plot of $\Delta R_f^\circ(MClO_4, MClO_3) = [\frac{1}{2}\Delta H_f^\circ(MClO_4) + \frac{1}{2}\Delta H_f^\circ(MClO_3) - \Delta H_f^\circ(ClO_3) - \frac{1}{2}\Delta H_f^\circ(M_2O)]$, y axis vs. $[\Delta H_f^\circ(MCl) - \frac{1}{2}\Delta H_f^\circ(M_2O)]$, x axis

of $MClO_3$ to MCl (Reaction 3). Thus, $\Delta F_f^\circ(MClO_3)$ may be computed for $LiClO_3$ and $CsClO_3$ from the equation:

$$\Delta F_f^\circ(MClO_3) = T\Delta S_f^\circ + \Delta F_f^\circ(MCl) - (\Delta H_f^\circ(MCl) - \Delta H_f^\circ(MClO_3)) \quad (15)$$

and were calculated to be -45.1 and -72.9 kcal./mole, respectively, at 25°.

From the aggregate data on $\Delta H_f^\circ(MClO_3)$ and $\Delta F_f^\circ(MClO_3)$ at 25°, the entries in Table V were derived to characterize the decompositions of $MClO_3$ salts via the oxide (Reaction 16) or the chloride (Reaction 17) routes:



Thus,

$$\Delta F_f^\circ(16) = \frac{1}{2}\Delta F_f^\circ(M_2O) - \Delta F_f^\circ(MClO_3), \text{ and } \Delta F_f^\circ(17) = \Delta F_f^\circ(MCl) - \Delta F_f^\circ(MClO_3)$$

Inspection of Table V clearly shows that the chloride route yields the more thermodynamically favored final reaction state for the thermal decompositions of $MClO_3$ compounds. As was demonstrated with the corresponding perchlorate salts (31), the ultimate product distribution is determined by the relative thermodynamic stabilities of the chlorides and oxides on an equivalent basis. $LiClO_3$, like $LiClO_4$, can decompose so as to yield Li_2O as well as $LiCl$, and this is undoubtedly indicated by the Cl_2 contents of their evolved gaseous decomposition products.

Table III. Method of Hoppe (27) as Applied to the Alkali Metal Perchlorates (25°)

Compound	$\Delta H_f^\circ(MClO_4)_{\text{lit.}}^a$	$\Delta H_f^\circ(MClO_4)_{\text{calcd.}}^a$
$LiClO_4$	-91.7 (43)	-92.2 (26)
$NaClO_4$	-92.2 (53)	-95.4 (27)
$KClO_4$	-103.6 (53)	-103.0 (27)
$RbClO_4$	-103.9 (53)	-102.1 (27)
$CsClO_4$	-103.9 (53)	-106.9 (27)

^a Kcal./mole.

Table IV. $\Delta H_f^\circ(MClO_3)$ at 25° (Kcal./Mole)

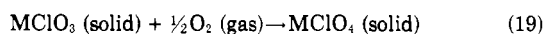
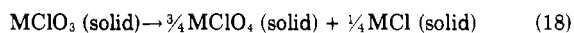
Compound	$\Delta H_f^\circ(MClO_3)_{\text{lit.}}(53)$	$\Delta H_f^\circ(MClO_3)_{\text{calcd.}}$
$LiClO_3$...	-70.0
$NaClO_3$	-85.7	-85.4
$KClO_3$	-93.5	-94.4
$RbClO_3$	-93.8	-93.5
$CsClO_3$...	-96.0

Table V. Thermodynamic Parameters (Kcal./Mole at 25°) for the Final Decomposition States of $MClO_3$ Compounds

Compound	$\Delta F_f^\circ^a$	$\Delta H_f^\circ^a$	$\Delta F_f^\circ^b$	$\Delta H_f^\circ^b$
$LiClO_3$	-21.8°	-1.2°	-46.8°	-27.7°
$NaClO_3$	14.2	36.0	-32.7	-12.5
$KClO_3$	31.1	53.0	-28.3	-10.7
$RbClO_3$	33.0	54.4	-30.7	-9.1
$CsClO_3$	40.4°	58.0°	-26.6°	-7.5°

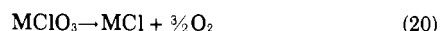
^a Reaction 16. ^b Reaction 17. ^c Estimated values.

Of interest in resolving the reaction sequences of MClO_3 compounds are the two additional general reactions, viz.,

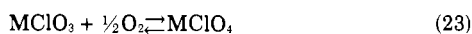


The pertinent thermodynamic data for these reactions are given in Table VI.

The close similarity in numerical values for ΔF° (18) and ΔH° (18) is to be expected for a completely solid phase reaction inasmuch as there is little or no loss in the number of degrees of vibrational freedom contributing to the heat capacity of the system as a result of the chemical change, i.e., ΔS° (18) \cong 0. However, the most surprising result of Table VI is the indication that direct oxygenation of chlorates to perchlorates appears possible (Reaction 19). Reaction 18 may be resolved into two simpler processes, viz.,

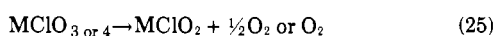
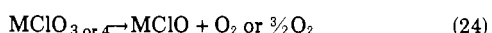


Thus, from Table VI a thermodynamic basis is available to support the contention that reversible interconversion of MClO_3 and MClO_4 compounds as per:

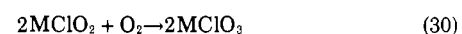
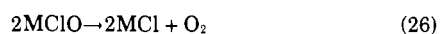


might be a significant step in the thermal decompositions of these materials (21, 56, 57). This assumes that $\Delta F^\circ(\text{MClO}_3)$ and $\Delta F^\circ(\text{MClO}_4)$ maintain the same relative values from 25° to reaction temperatures.

Measurable quantities of the lower halates (MClO , MClO_2) have never been reported from decomposition studies of MClO_3 and MClO_4 salts, thereby suggesting that reactions such as:



probably do not play an important role; rather the reverse reaction type seems to be true inasmuch as the pyrolysis of MClO and MClO_2 compounds usually follow a course leading to transient MClO_3 formation (1, 24). The latter would therefore indicate substantially irreversible internal oxygenation effects like those indicated below:



The present studies show that LiClO_3 melts (maintained at some temperature T_1) can accumulate considerable quantities of LiClO_4 during thermal decomposition; on the other hand, LiClO_3 achieving a measurable rate of pyrolysis (at some temperature T_2 , $T_2 > T_1$) yields only a small LiClO_3 content at any stage of decomposition (36). Similar results have been found in investigations of the decomposi-

tions of KClO_3 (20, 21, 23, 25, 50) and of KClO_4 (4, 21, 22, 23, 25, 49, 56). These observations undoubtedly stem from the greater thermodynamic stabilities of MClO_4 salts as compared to the corresponding MClO_3 compounds (Table VI), i.e., the forward of Reaction 23 is favored over the reverse reaction, and from the greater kinetic stabilities of perchlorates over chlorates. The latter point was readily demonstrated in the present work for LiClO_3 in comparison with LiClO_4 , and has been found to be true for MClO_3 and MClO_4 compounds in general (40). The ultimate pyrolysis of LiClO_4 to LiCl which produces LiClO_3 as an intermediate (36) through the rate-controlling reaction $\text{LiClO}_4 (\text{liquid}) \rightarrow \text{LiClO}_3 (\text{liquid}) + \frac{1}{2} \text{O}_2 (\text{gas})$ is due to the rapid irreversible decomposition of LiClO_3 to LiCl (Reaction 17). The trends in the available thermodynamic and kinetic data would suggest that the behavior observed with LiClO_3 and LiClO_4 also prevails for the other MClO_3 and MClO_4 compounds. The preparation of pure chlorates from decomposing perchlorates though apparently possible at low partial pressure of oxygen for the heavier alkali metals (Table VI) does not appear feasible because of the simultaneous intervention of Reaction 17 with the reverse of Reaction 19. Similarly, the complete conversions of chlorates into perchlorates as per the composite Reaction 22 seems unlikely unless the rate of oxygen production (Reaction 20) is less than the rate of chlorate oxygenation (Reaction 21), a circumstance which does not appear to hold for either LiClO_3 or KClO_3 (16, 25).

Despite the indications from Table VI that direct oxygenation by molecular oxygen of MClO_3 to MClO_4 is thermodynamically possible at low temperatures and partial pressures of oxygen, this conversion has not been observed by mere exposure of MClO_3 to O_2 . Thus, the treatment of KClO_3 at 475° with 1200 atmospheres O_2 pressure did not result in formation of KClO_4 (14). In the present study, maintaining samples of pure LiClO_3 , 80 mole % LiClO_3 -20 mole % LiClO_4 , and 80 mole % LiClO_3 -10 mole % LiClO_4 -10 mole % LiCl at 150° for two days under 100 atmospheres O_2 pressure resulted in no change in the compositions of these samples. Thus, it seems likely that the MClO_3 - MClO_4 conversion (Reaction 23) is achieved through atomic oxygen (21, 22, 23, 57). As a result the circumstances prevailing in a melt of decomposing chlorate cannot be readily duplicated in the laboratory. However, it is of interest to note that up to 350°, the rate of decomposition of KClO_3 to KCl and O_2 in KClO_3 - MnO_2 mixtures was greatly retarded by application of high O_2 pressures (45). Decomposition of the KClO_3 had apparently only been followed by analyses for KCl , so that the possibility of enhanced KClO_4 formation under these conditions by Reaction 23, unfortunately, could not be tested.

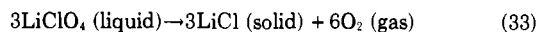
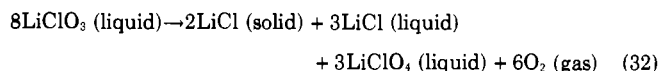
The exothermic decomposition portion of the DTA curve of LiClO_3 (Figure 2a) can be resolved into its component parts by further consideration of the TGA and the heat of formation data for this compound. As seen, the TGA pattern (Figure 3a) delineates two major stages of weight loss and it is to be anticipated that these overall changes

Table VI. Thermodynamic Parameters (Kcals./Mole at 25°) for MClO_4 Formation from MClO_3 Compounds

Compound	ΔF° ^a	ΔH° ^a	ΔF° ^b	ΔH° ^b
LiClO_3	-23.3°	-23.2°	-15.4°	-21.7°
NaClO_3	-8.6	-8.0	-0.5	-4.1
KClO_3	-9.5	-10.3	-3.4	-10.1
RbClO_3	-11.7	-9.8	-5.4	-10.1
CsClO_3	-7.0°	-7.7°	-0.4°	-7.9°

^a Reaction 18. ^b Reaction 19. ^c Estimated values.

will also be manifested in the DTA curve of LiClO_3 in terms of the following reactions:



A saturated solution of LiCl in LiClO_4 at about 425° is of approximately a 1:1 mole ratio of components (36) and this composition was used to estimate the phase distribution resulting in Reaction 32. Assuming that the changes represented by Equations 32 and 33 occur at an average temperature of 425° , values of ΔH° may be computed for these reactions. In the calculations, enthalpy changes due to solution effects are neglected. $\Delta H^\circ_f(\text{LiClO}_3)_{\text{liquid}}$ is taken to be -68.0 kcal./mole on the assumption that the entropy of fusion of LiClO_3 is 5 e.u. and, therefore, $\Delta H^\circ_{\text{fusion}}(\text{LiClO}_3) = T_{\text{m.p.}} \Delta S^\circ_{\text{fusion}}(\text{LiClO}_3) = 2.0$ kcal./mole (60). Values of $\Delta H^\circ_f(\text{LiCl})_{\text{liquid and solid}}$ and $\Delta H^\circ_f(\text{LiClO}_4)_{\text{liquid}}$ are available for 425° (15). The calculations show ΔH°_f (Reaction 32) = -175.2 kcal. and ΔH°_f (Reaction 33) = -46.2 kcal. which coincide roughly with the relative sizes of the two exothermic breaks found in the DTA curve of LiClO_3 (Figure 2a). The high degree of heat loss caused by sample dispersal and decreased sample mass in contact with the thermocouple can be gauged by comparing the second exotherm in Figure 2a with the corresponding exotherm from the DTA of 0.73 grams of a mixture of LiCl and LiClO_4 in 5:3 mole ratio, i.e., the residual product produced by reaction (32) during the DTA of one gram LiClO_3 . It was found that this mixture yielded a rather coherent reaction residue with little sample splattering evident, and that the final LiCl fusion endotherm agreed well in area with that obtained by DTA of 0.47 gram LiCl . Thus, the ratio of areas of the second exotherm in Figure 2a to that from the synthetic LiClO_4 - LiCl mixture was about 1:3.

The effects of thermal overlap of successive reactions during DTA and the role that the heating rate plays in this phenomenon are of interest. At $10^\circ/\text{min.}$ heating rate (Figure 1a), no resolution of the decomposition sequence was found, but such a differentiation did appear at $4^\circ/\text{min.}$ heating rate (Figure 2a). Observe that the peak exothermal temperature recorded in Figure 1a is about 445° , whereas that in Figure 2a is only about 425° . Apparently, at the higher heating rate, during decomposition, the sample can attain higher temperatures than at the lower heating rate, so that Reactions 32 and 33 can occur simultaneously at appreciable rates. However, at the lower heating rate there is less sample selfheating and thus a clearer definition of reactions of differing rates. Therefore, the degree of thermal overlap is greater at the higher heating rate than at the lower heating rate (Figure 6). At the proper heating rate, the TGA method does not appear to suffer appreciably from the shortcoming of overlapping of the effects of successive reactions (Figure 3a). Those approaches developed for securing quantitative kinetic data from dynamic DTA (6) and TGA (19) experiments do not seem applicable to chlorate salts due to the factors of large thermal transients and to the occurrence of multiple reaction paths.

Analyses of the Cl-O bonding characteristics in ClO_x^- ions ($x = 1, 2, 3, 4$) have shown the extent of π -bonding, originating from the 3d orbitals of chlorine, to be in the order (11, 51, 59): $\text{ClO}_4^- > \text{ClO}_3^- > \text{ClO}_2^- > \text{ClO}^-$. For the LiClO_x compounds, as well as for MClO_x compounds in general, the observed order of thermal stabilities is $\text{MClO}_4 > \text{MClO}_3 > (\text{MClO}_2, \text{MClO})$. It has been found that the pyrolyses of MClO_3 salts results in the intermediate

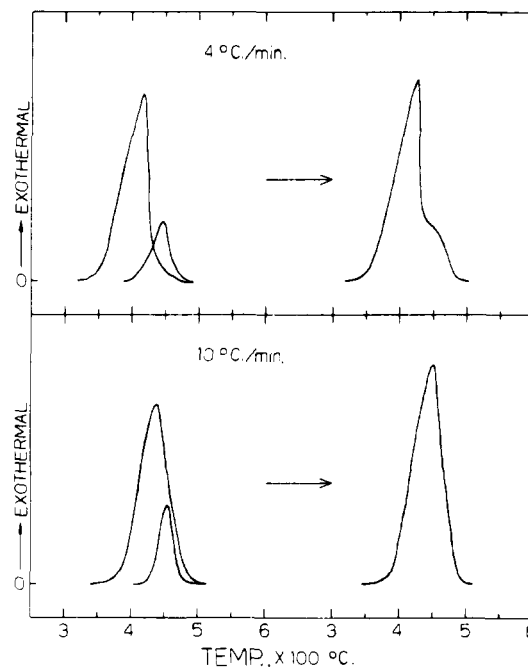


Figure 6. Thermal overlap of successive reactions during DTA

formation of MClO_4 , and that the decompositions of MClO_2 and MClO involve transient MClO_3 formation. Thus, a portion of the thermal breakdown of the lower MClO_x compounds ($x < 4$) is accompanied by a transition of these oxyanions to states of higher degrees of π -bonding.

ACKNOWLEDGMENT

Thanks are extended to John E. Ricci of New York University for a number of stimulating discussions pertaining to this work.

LITERATURE CITED

- Addison, C.C., "Supplement to Mellor's Comprehensive Treatise on Inorganic and Theoretical Chemistry," Supplement II, Part I, pp. 538-539, Longmans, Green, London, 1956.
- Anderson, D.A., Freeman, E.S., *Nature* **195**, 1297 (1962).
- Berg, L., *Z. anorg. u. allgem. Chem.* **155**, 311 (1926); **166**, 231 (1927); **181**, 131 (1929).
- Bircumshaw, L.L., Phillips, T.R., *J. Chem. Soc.* **1953**, p. 703.
- Borchardt, H.J., Daniels, F., *J. Phys. Chem.* **61**, 917 (1957).
- Borchardt, H.J., Daniels, F., *J. Am. Chem. Soc.* **79**, 41 (1957).
- Brown, F.E., Burrows, J.A., McLaughlin, H.M., *Ibid.* **45**, 1343 (1923).
- Bruehl, H., *Bull. soc. ind. min.* **35**, 155 (1912).
- Burrows, J.A., Brown, F.E., *J. Am. Chem. Soc.* **48**, 1790 (1926).
- Campbell, A.N., Griffiths, J.E., *Can. J. Chem.* **34**, 1647 (1956).
- Cartmell, E., Fowles, G.W.A., "Valency and Molecular Structure," pp. 179-180, Academic Press, New York, 1956.
- Clapper, T.W., Gales, W.A., Schumacher, J.C., "Perchlorates: Their Properties, Manufacture, and Uses," Schumacher, de Barry Barnett, E., Wilson, G.L., "Inorganic Chemistry," 2nd ed., pp. 538-539, Longmans, Green, London, 1959.
- Dodé, M., Basset, J., *Bull. soc. chim.* [5] **2**, 344 (1935).
- Dow Chemical Co., "Joint Army-Navy-Air Force Thermochemical Tables," Thermal Laboratory, Midland, Mich., (1960).
- Farmer, W., Firth, J.B., *J. Chem. Soc.* **125**, 82 (1924).
- Feigl, F., "Qualitative Analysis by Spot Tests: Inorganic and Organic Applications," 3rd ed., pp. 128-129, 114-115, Elsevier, New York, 1947.
- Freeman, E.S., Anderson, D.A., *Nature* **199**, 63 (1963).

- (19) Freeman, E.S., Carroll, B., *J. Phys. Chem.* **62**, 394 (1958).
 (20) Geidis, J.M., Rochow, E.G., *J. Chem. Educ.* **40**, 78 (1963).
 (21) Glasner, A., Weidenfeld, L., *J. Am. Chem. Soc.* **74**, 2464, 2467 (1952).
 (22) Harvey, A.E., Edmison, M.T., Jones, E.D., Seybert, R.A., Catto, C.H., *Ibid.* **76**, 3270 (1954).
 (23) Harvey, A.E., Wassink, C.J., Rodgers, T.A., Stern, K.H., *Ann. N. Y. Acad. Sci.* **78**, 971 (1960).
 (24) Heslop, R.B., Robinson, P.L., "Inorganic Chemistry: A Guide to Advanced Study," pp. 380-384, Elsevier, New York, 1960.
 (25) Hofmann, K.A., Marin, P.H., *Sitzber. preuss. Akad. Wiss. Physik.-math. Klasse* **27**, 448 (1932).
 (26) Hoppe, R., private communication.
 (27) Hoppe, R., *Z. anorg. u. allgem. Chem.* **296**, 104 (1958).
 (28) Kireev, V.A., *J. Gen. Chem. U.S.S.R.* **16**, 1199 (1946).
 (29) Kraus, C.A., Burgess, W.M., *J. Am. Chem. Soc.* **49**, 1225 (1927).
 (30) Markowitz, M.M., *J. Chem. Educ.* **33**, 36 (1956).
 (31) Markowitz, M.M., *J. Inorg. Nucl. Chem.* **25**, 407 (1963).
 (32) Markowitz, M.M., *J. Phys. Chem.* **62**, 827 (1958).
 (33) Markowitz, M.M., Boryta, D. A., *Anal. Chem.* **32**, 1588 (1960).
 (34) Markowitz, M.M., Boryta, D.A., *J. Chem. Eng. Data* **7**, 586 (1962).
 (35) Markowitz, M.M., Boryta, D.A., *J. Phys. Chem.* **64**, 1711 (1960).
 (36) *Ibid.* **65**, 1419 (1961).
 (37) *Ibid.* **66**, 358 (1962).
 (38) Markowitz, M.M., Boryta, D.A., Capriola, G., *J. Chem. Educ.* **38**, 96 (1961).
 (39) Markowitz, M.M., Boryta, D.A., Harris, R.F., *J. Phys. Chem.* **65**, 261 (1961).
 (40) Markowitz, M.M., Boryta, D.A., Stewart, H., Jr., unpublished results.
 (41) Markowitz, M.M., Harris, R.F., *J. Phys. Chem.* **63**, 1519 (1959).
 (42) Markowitz, M.M., Harris, R.F., Hawley, W.N., *J. Inorg. Nucl. Chem.* **22**, 391 (1961).
 (43) Markowitz, M.M., Harris, R.F., Stewart, H., Jr., *J. Phys. Chem.* **63**, 1325 (1959).
 (44) Markowitz, M.M., Stewart, H., Jr., Boryta, D.A., *Inorg. Chem.* **2**, 768 (1963).
 (45) McLaughlin, H.M., Brown, F.E., *J. Am. Chem. Soc.* **50**, 782 (1928).
 (46) Mellor, J.W., "Comprehensive Treatise on Inorganic and Theoretical Chemistry," Vol. I, p. 360, Longmans, Green, London, 1922.
 (47) Meyer, M., *J. Chem. Educ.* **17**, 494 (1940).
 (48) Mylius, F., Funk, W., *Ber.* **30**, 1720 (1897).
 (49) Otto, C.E., Fry, H.S., *J. Am. Chem. Soc.* **45**, 1134 (1923).
 (50) *Ibid.* **46**, 269 (1924).
 (51) Palmer, H.G., "Valency: Classical and Modern," 2nd ed., p. 154, Oxford Univ. Press, New York, (1959).
 (52) Potilizin, A., *J. Russ. Phys. Chem. Soc.* **16**, 840 (1883).
 (53) Rossini, F.D., Wagman, D.D., Evans, W.H., Levine, S., Jaffe, J., *Natl. Bur. Std. (U.S.)*, Circ. 500, (1952).
 (54) Schechter, W.E., Miller, R.R., Bovard, R.M., Jackson, C.B., Pappenheimer, J.R., *Ind. Eng. Chem.* **42**, 2348 (1950).
 (55) Sidgwick, N.V., "The Chemical Elements and Their Compounds," Vol. II, p. 1205, Oxford Univ. Press, New York, 1950.
 (56) Simchen, A.E., *J. Phys. Chem.* **65**, 1093 (1961).
 (57) Stern, K.H., Bufalini, M., *Ibid.* **64**, 1781 (1960).
 (58) Treadwell, F.P., Hall, W.T., "Analytical Chemistry," Vol. II, 9th English ed., pp. 183-184, John Wiley, New York, 1942.
 (59) Wagner, E.L., *J. Chem. Phys.* **37**, 751 (1962).
 (60) Wenner, R.R., "Thermochemical Calculations," pp. 23-26, McGraw-Hill, New York, 1941.

RECEIVED for review February 18, 1964. Accepted May 6, 1964.

Isomeric Bis(Vinylphenyl)borinic Acids

WESLEY J. DALE¹ and JAMES E. RUSH²

Department of Chemistry, University of Missouri, Columbia, Mo.

The synthesis of bis(*o*-, *m*-, and *p*-vinylphenyl)borinic acids, isolated as their 2-aminoethyl esters, is reported. The bis(*o*- and *m*-vinylphenyl)borinic acids were obtained as uncrystallizable oils by hydrolysis of their esters. The para isomer could not be isolated in monomeric form.

THE AUTHORS described, in a recent paper (1), the synthesis of the isomeric vinylbenzeneboronic acids and now wish to report the synthesis of the corresponding bis(*o*-, *m*-, and *p*-vinylphenyl)borinic acids.

Both bis(*o*-vinylphenyl)borinic acid and the corresponding meta isomer were prepared by allowing 2 moles of *o*(or *m*)-vinylphenylmagnesium bromide to react with 1 mole of butyl borate at low temperature. The reaction mixture was hydrolyzed with dilute hydrochloric acid, and the product was isolated from the ethereal solution as the 2-aminoethyl ester. This method of isolation was more advantageous than attempts to isolate the free acid.

Both esters were readily hydrolyzed in the presence of dilute hydrochloric acid, yielding the free acids as viscous oils which could not be induced to crystallize. All attempts to dehydrate the acids led to polymer formation exclusively.

An initial attempt to synthesize bis(*p*-vinylphenyl)borinic acid by the method employed for the ortho and meta isomers met with remarkable success; a 58% yield of the crude 2-aminoethyl ester was obtained, which melted at 170-175°C. This result could not be repeated, however; only polymeric material was isolated in each additional attempt. However, when hydrolysis was effected with an aqueous solution of ammonium chloride, a 35% yield of the ester was obtained. Alternately, this ester could be obtained (35%) by treating the reaction mixture with an excess of 2-aminoethanol rather than with aqueous ammonium chloride. No attempt was made to isolate the free acid.

¹ Present address: National Science Foundation, Washington, D. C.

² Present address: Chemical Abstracts Service, Ohio State University, Columbus, Ohio.